2024 IEEE/RSJ International Conference on Intelligent Robots and Systems (IROS)
October 14-18, 2024. Abu Dhabi, UAE

A Soft Robotic Finger Inspired by Biological Perception Models for Tactile Sensing

Baijin Mao, Qiangjing Yuan, Yuyaocen Xiang, Kunyu Zhou, Weichen Wang,
Yaozhen Chen, Hongwei Hao, and Juntian Qu*

***Abstract*— Tactile sensing is pivotal for enabling effective human-robot interaction, especially in unstructured environments. This work introduces an innovative bioinspired soft robotic finger endowed with shape-adaptive and multi-modal tactile perception capabilities, drawing inspiration from diverse biological tactile sensing modalities. Through an advanced Fin Ray structure, the soft finger features tactile whiskers on its fingertips, facilitating perception of obstacle orientation, fingertip pressure, surface roughness, and grasping ball size. Leveraging distributed optical fiber sensing technology, we develop a sophisticated multi-point, multi-modal tactile perception neural network tailored for the soft finger. Meticulous integration via advanced 3D printing and silicone coating techniques seamlessly embeds optical fiber sensors within the soft robotic finger, creating an intelligent perception-capable bioinspired mechanical system. Experimental validation confirms the soft robotic finger's sensitive and precise force perception and curvature recognition abilities, achieving accuracies of up to 100%. In summary, our bioinspired robotic finger holds significant promise for applications in intelligent sensing, non-destructive grasping, and fruit classification within unstructured environments, thus advancing the field of robotics and human-robot interaction.**

I. INTRODUCTION

Soft grippers endowed with tactile sensing capabilities hold profound promise in the realm of human-robot interaction [1]–[3]. Tactile sensors distributed throughout soft grippers facilitate the acquisition of multi-modal sensory data within unstructured environments [4], [5], encompassing diverse parameters such as contact states, surface attributes, and physical properties. This tactile information plays a pivotal role in enhancing the dexterity of robotic operations. In recent year, a plethora of researchers, both domestically and internationally, have embarked on extensive investigations within the realm of tactile sensing technology applied to soft grippers [6].

However, the prevailing approach adopted by most researchers involves the utilization of either singular sensors or arrays of multiple sensors to realize the tactile perception functionality of soft robotic manipulators [7], [8]. However, such methodologies are beset by two primary challenges: (1) Singular tactile sensors yield limited tactile perception information, thereby impeding the comprehensive acquisition of tactile information and imposing operational constraints during human-machine interactions; (2) While the utilization of multi-sensor arrays facilitates the acquisition of a broader spectrum of tactile perception data, it often entails the deployment of intricate and redundant electronic circuits, leading to issues related to system complexity, low integration levels, and compromised reliability. Consequently, the development of a tactile sensing system capable of acquiring multi-modal tactile perception data while maintaining high integration and reliability emerges as a formidable challenge in the current landscape.

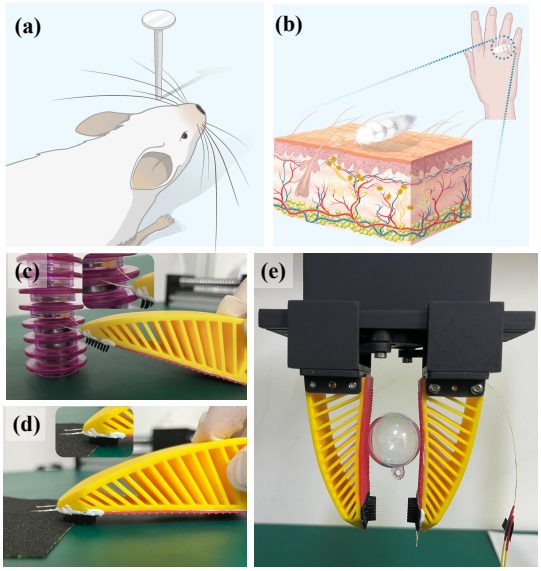

Fig. 1. (a) Mouse whiskers make contact with an obstacle. (b) Finger hairs perceive the descent of the feather. (c) The bionic finger touches an obstacle. (d) The bionic finger glides across a sandpaper. (f) Grasping a ball.

To tackle the aforementioned challenges, as depicted in Figure 1, we have seamlessly fused the tactile perception mechanisms of rat vibrissae and human fingertip hairs into a soft robotic finger, introducing a novel soft structure that amalgamates various biological tactile sensing principles. The finger not only simulates the rat's whiskers to perceive the surrounding environment and detect obstacles but also mimics the human skin and hairs to perceive tactile information about the surface of touched objects. To address the chal-

*J. Qu is the corresponding author. E-mail: juntian.qu@sz.tsinghua.edu.cn
This work was supported by the Shenzhen "Pengcheng Peacock Program", the Beijing "Youth Talent Promotion Project", the Tsinghua SIGS Cross-disciplinary Research and Innovation Fund (grant no. JC2022002), the Shenzhen Science and Technology Program (grant no. WDZC20231128114452001), the Tsinghua SIGS Overseas Research Cooperation Fund (grant no. HW2023001), the Tsinghua SIGS Scientific Research Startup Fund (grant no. QD2022021C), the Jianghuai Dream Fund (grant no. 2023 - ZM 01 Z006), and the Shenzhen Key Laboratory of Advanced Technology for Marine Ecology (grant no. ZDSYS20230626091459009).

lenges posed by complex, non-integrable, and low-precision sensing systems, we have adeptly adopted fiber Bragg gratings (FBGs) tactile sensors to construct a distributed sensing tactile perception system. Fiber Bragg grating sensors offer numerous advantages [9] over conventional mechanical and electronic sensors, including high sensitivity, immunity to electromagnetic interference, corrosion resistance, and so on. Particularly noteworthy is their distributed sensing capability [10], [11], which allows the integration of multiple sensors within a single optical pathway, contrasting sharply with traditional single-point monitoring methods that suffer from both economic inefficiency and inadequate performance. These attributes collectively offer a robust solution for the highly integrated and multimodal sensing system required for the tactile perception system of the soft finger. In summary, the highlights of this study are outlined as follows:

(1) Drawing inspiration from a variety of biological tactile perception models found in nature, we have conceived and designed a novel configuration for a multi-modal tactile perception mechanical finger, integrating biomimetic vibrissae, skin, and hairs.

(2) Diverging from conventional robotic fingers with single-mode tactile perception, our proposed finger system achieves a high degree of integration with multi-modal tactile perception capabilities. It can effectively sense multimodal information, including the direction of beard touch, fingertip force, roughness, and object grasping size. This augmentation significantly enhances the convenience and reliability of human-machine interactions.

The subsequent sections of the paper are organized as follows: Section II presents a review of related research work. Section III details the design and fabrication process of the bionic finger. Section IV encompasses the experimental validation, confirming the soft robotic finger's proficiency in sensing multimodal information. Finally, Section V offers a comprehensive summary and discussion of the findings of this work.

II. RELATED WORKS

Recently, there has been significant progress in tactile sensing technology applied to soft robotics. It plays pivotal roles in fruit picking, non-destructive handling, medical rehabilitation, and underwater exploration. For instance, Li et al. employed a vision-tactile approach in a universal jamming gripper to achieve high-quality tactile sensing [12]. Xie et al. embedded EGaIn-based soft sensors in a soft tentacle gripper to provide sensory feedback on elongation and expansion induced by pneumatic inflation [13]. Luo et al. proposed the digital fabrication of pneumatic actuators with integrated sensing through machine weaving, enabling automatic programming of actuator bend during inflation [14]. Sun et al. utilized hydrogel sensors to identify thermal stimuli and mechanical deformation of soft actuators through machine learning methods [15]. Dilibal et al. developed a monoblock soft robotic gripper with three geometrically gradient fingers equipped with soft force sensors [16]. Shen et al. presented a soft gripper integrated with a hydrogel strain sensor capable

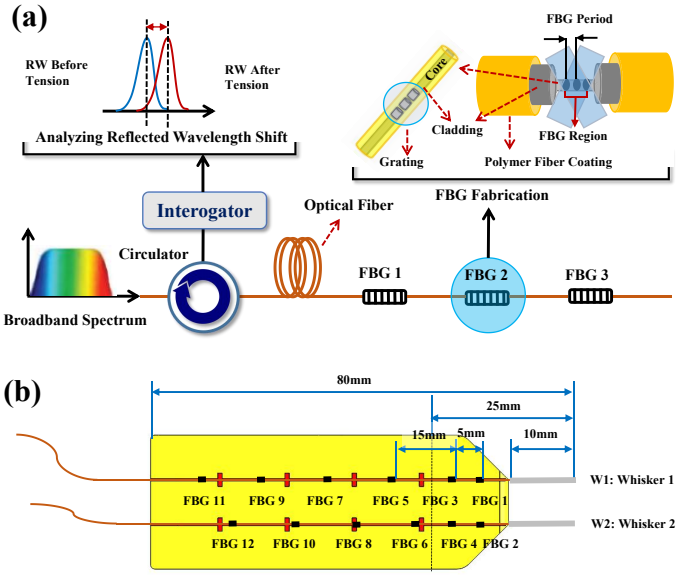

Fig. 2. (a) The construction and principle of the fiber Bragg grating sensing System. (b) The layout of FBGs embedded in the soft finger.

of autonomously sensing bending angles and discriminating object sizes [17]. Moreover, to accurately detect force under unstructured environments, FBGs have been widely employed in robotic grippers [18], [19]. Park et al. developed an exoskeletal force-sensing robot finger by embedding FBG sensors into a polymer-based structure [20]. Similarly, Park et al. described a two-fingered dexterous hand incorporating optical fibers for accurate force sensing and estimation of contact locations [21]. Kim et al. proposed a robotic end-effector with force sensing through FBG sensors [22]. Feng et al. introduced a roughness recognition sensor for robotic fingertips based on FBGs [23], while Massari developed a robotic gripper utilizing FBGs for tactile feedback [24].

In contrast to previous studies, we propose a highly integrated fiber optic sensing system that leverages distributed sensing technology and amalgamates various tactile perception biological models. This novel robotic finger is capable of discerning multiple tactile information cues.

III. DESIGN AND FABRICATION

A. Fiber Bragg grating sensing mechanism

Fiber Bragg grating is a type of optical passive component renowned for its wavelength modulation capability. The core sensing mechanism of FBG is illustrated in Figure 2(a). Generally, a fiber-optic sensing setup typically includes a circulator, interrogator, light source, and optical fibers. In this study, we utilized a commercially available integrated fiber demodulator (X152, Micronor) to establish the sensing system. FBG fabrication involves exposing a small section of photosensitive fiber to an optical wave with a periodic intensity distribution, achieved through holographic interference or phase mask techniques. The fiber comprises three primary components: the core, cladding, and buffer coating. The cladding serves to reflect stray optical waves back into the

core, minimizing transmission loss. FBG sensors represent one of the most extensively used and versatile types of fiber optic sensors, capable of modulating the wavelength of reflected light waves in response to variations in ambient temperature or strain.

The reflected signal is called center wavelength λ_B that can be given as

$$\lambda_B = 2n_{eff} \cdot \Lambda \tag{1}$$

Where n_{eff} is the effective refraction index of the optical fiber, and Λ is the grating spatial period. The relationship between the wavelength shift and the strain is given as [25]

$$\frac{\Delta\lambda_B}{\lambda_B} = (1 - P_e)\,\varepsilon + (\alpha_A + \alpha_n)\Delta T \tag{2}$$

$$P_e = \frac{n_{eff}^2}{2}\left[P_{12} - v\,(P_{11} + P_{12})\right] \tag{3}$$

where P_e is the strain optic coefficient which is a fixed value for a the specific types of fiber, α_A is the thermal expansion coefficient, α_n is the thermo-optic coefficient, v is Poisson's coefficient, and P_{11} and P_{12} are Pockel's coefficients of the strain optical tensor. Strain (ε) and temperature (ΔT) are variables that are independent of each other. Thus, there is a linear relationship between λ_B and ε. Ignoring the temperature effect, the relationship between the FBG wavelength and strain. Similarly, there is also a linear relationship between λ_B and temperature if only the strain is considered. In this work, the demodulator incorporates an internally integrated temperature-compensated FBG with a central wavelength of 805 nm, along with an automated compensation algorithm. All experiments are conducted in a temperature-controlled environment, eliminating the need for additional temperature compensation measures.

B. Bionic finger design

Drawing inspiration from studies on fish fin bone structure and shapes [26], the Fin Ray effect stands out as a quintessential example of a passive adaptive soft gripper [27]. To endow the biomimetic soft robotic finger with passive adaptability, we employ the Fin Ray structure as its primary framework. As illustrated in Figure 3, the primary structure of the bionic finger is predicated on the optimized design proposed by Elgeneidy [28]. Through iterative improvements in design [29], the soft finger (Figure 1(e)) demonstrates remarkable proficiency in detecting variations in curvature when grasping objects of varying sizes.

To enable the biomimetic finger with multimodal tactile perception capabilities, as depicted in Figure 2b, we integrate two optical fibers spaced 10 mm apart into the soft finger to replicate the intricate tactile sensing mechanisms observed in human fingers. Each fiber hosts 6 distributed FBG sensors. The central wavelengths of the FBGs numbered 1-12 are about 861.7nm, 858.7nm, 855.6nm, 852.7nm, 844.1nm, 841.0nm, 838.1nm, 835.0nm, 832.0nm, 829.0nm, 825.9nm, and 822.8nm. Drawing inspiration from the tactile perception mechanism of rat whiskers, we incorporate two biomimetic whiskers at the fingertip to emulate the acute environmental

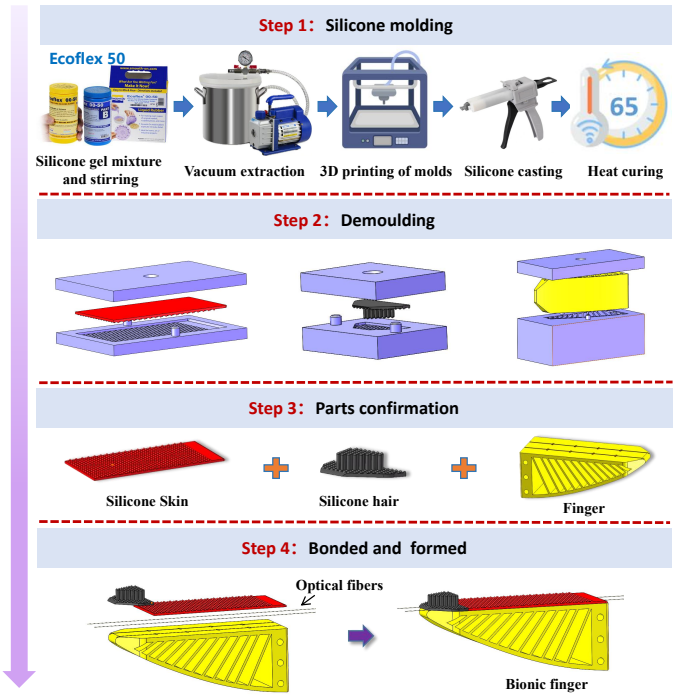

Fig. 3. Manufacturing process flow of the bionic soft finger

perception and obstacle detection observed in rat whiskers. Two 10 mm optical fibers extension from the fingertip are uniformly coated with a silicone layer to mimic this biological modal. Similar to the cantilever force model, when the whiskers encounter an object, their base experiences the greatest force. Hence, we position two FBGs at the base of each whisker.

Moreover, biomimetic fingertip hairs are added to the fingertip to replicate the tactile perception abilities of human skin and hairs. These hairs not only increase frictional force by enlarging the contact area for better surface roughness perception but also allow for the sense of frictional force direction through bending. To maintain basic rigidity and strength while avoiding excessive hardness, we opt for a hardness of 60A, with a length half that of the whisker and a diameter of 1mm. In addition, to maximize hair density, a total of 42 biomimetic hairs are arranged in a triangular pattern at the fingertip. The biomimetic skin surface is textured with numerous protrusions, primarily enhancing finger grip friction. To balance soft finger flexibility with tactile sensitivity beneath the skin surface, the biomimetic skin thickness is set at 1mm [30], with a low hardness of 20A.

C. Fabrication

The fabrication process of the bionic soft finger involves four main steps: silicone molding, demolding, testing and confirmation, and parts bonding. Utilizing Ecoflex silicone sourced (Smooth-On, USA) as the primary raw material, the bionic soft finger is crafted with distinct hardness levels for its main structure, bionic skin, and bionic hairs, set at 50A, 20A, and 60A, respectively.

Initially, the AB silica gel is mixed and poured into a measuring cup, maintaining an equal ratio of 1:1, before being thoroughly stirred. Following this, the homogenously mixed silica gel undergoes a vacuuming process to expel any trapped air bubbles. Once the vacuum treatment is completed, the prepared silicone is carefully loaded into a specialized glue gun. With precision, the silicone is slowly extruded into the intricately designed 3D printing mold via the glue gun. The fabrication process proceeds through a series of steps. Firstly, the silicone-filled mold is subjected to curing in a 65 °C oven for an hour, ensuring optimal material cohesion and structure formation. Upon natural cooling, the crafted soft finger undergoes a precise demolding process, meticulously removing any excess silicone. Subsequently, the demolded parts are subjected to a careful inspection, scrutinizing for any potential defects.

In the final phase, meticulous assembly of the finger, bionic skin, bionic whiskers, and optical fiber is achieved using a specialized silicone adhesive. These executed sequential procedures culminate in the fabrication of the bionic soft finger, ensuring precision, reliability, and functionality.

IV. Results and Discussions

To evaluate the tactile sensing capabilities of the bionic robotic finger, we have conducted three systematic experiments: (1) Directional sensing of bionic whiskers, (2) Tactile sensing assessment of bionic hairs, and (3) Performance of tactile sensing using a soft gripper based on the bionic finger.

A. Direction sensing of the whiskers

To validate the directional sensing capability of the bionic whiskers, we initially constructed an optic-fiber sensing system (Figure 2) with a demodulation frequency of 200 Hz and subsequently employed LABVIEW for data acquisition. As depicted in Figure 4(a), the bionic whiskers exhibit three distinct states: State 1 (S1) represents the natural state where the tentacle remains untouched; State 2 (S2) and State 3 (S3) depict the bending states occurring in opposite directions when the whiskers encounter an obstacle or undergo stress.

Examining Figure 4(b), prior to 2.5 s, it is evident that the wavelengths of FBG1 and FBG2 remain relatively stable when whisker 1 (W1) and whisker 2 (W2) are in State 1 (S1). Upon W1 suddenly making contact with an obstacle and transitioning to State 3, the wavelength of FBG1 contracts, resulting in a negative change value. Conversely, when W2 unexpectedly encounters an obstacle and turns to State 2, the wavelength of FBG1 elongates, leading to a positive change value. Analogously, W2 demonstrates comparable tactile performance. Consequently, considering the interference threshold (0.004 nm), the directional states of the whiskers can be discerned through wavelength shifts.

The directional sensing of W1 and W2 operates independently without mutual interference, enabling simultaneous perception of different directions (e.g., 18s-20s). Furthermore, the response speed of the tentacles' directional sensing is rapid, transitioning from State 1 to either State 2 or State 3 within 0.5s. However, it is worth noting that the response speed is inherently constrained to some extent by the elasticity effect of the silicone material.

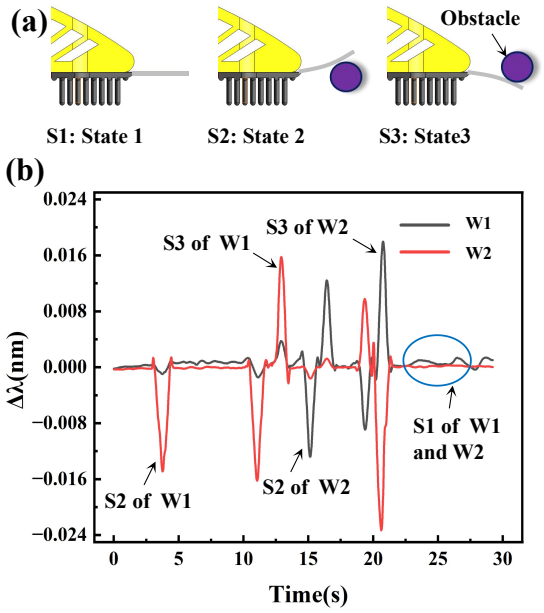

Fig. 4. (a) The schematic of the whisker direction sensing state. (b) Direction sensing of the whisker 1(W1) and whisker 2(W2).

B. The characteristics of fingertip tactile perception

1) Sense of pressure: Pressure sensing serves as the fundamental aspect of tactile perception. To assess the pressure sensing capabilities of the bionic finger's fingertip, as depicted in Figure 5(a), a force measurement system was established. The force measurement device utilized possesses a resolution of 0.005 N. In Figure 5(b), positive pressure was incrementally applied to the fingertip, starting from 0 up to 3 N, with a step size of 0.5 N and a duration of approximately 10 s for each step. Experimental observations indicate that the wavelength shift remains consistent when the positive pressure remains constant, indicating a high level of stability in fingertip force sensing. The relationship between fingertip pressure and wavelength shift is illustrated in Figure 5(c). The experiment demonstrates a linear correlation between fingertip pressure and the wavelength shifts of FBG1-FBG4. Notably, FBG1 exhibits the highest sensitivity, with a slope of 24.41, whereas FBG3 displays the lowest sensitivity, with a slope of 8.87.

2) Sense of roughness: The roughness test experiment of the bionic finger is depicted in Figure 6(a). The sandpaper is affixed to the moving table of the screw slide, while the base of the finger is securely attached to the holder. The bionic hairs make light contact with the sandpaper. Initially, 320-grit sandpaper is secured onto the moving table at varying speeds (0mm/s, 1mm/s, 2mm/s, 3mm/s). As illustrated in Figure 6(b) (FBG 1), there exists no discernible relationship between the speed and the wavelength drifts when the fingertip pressure remains constant. Consequently, the wavelength drift of FBG1 remains nearly unchanged.

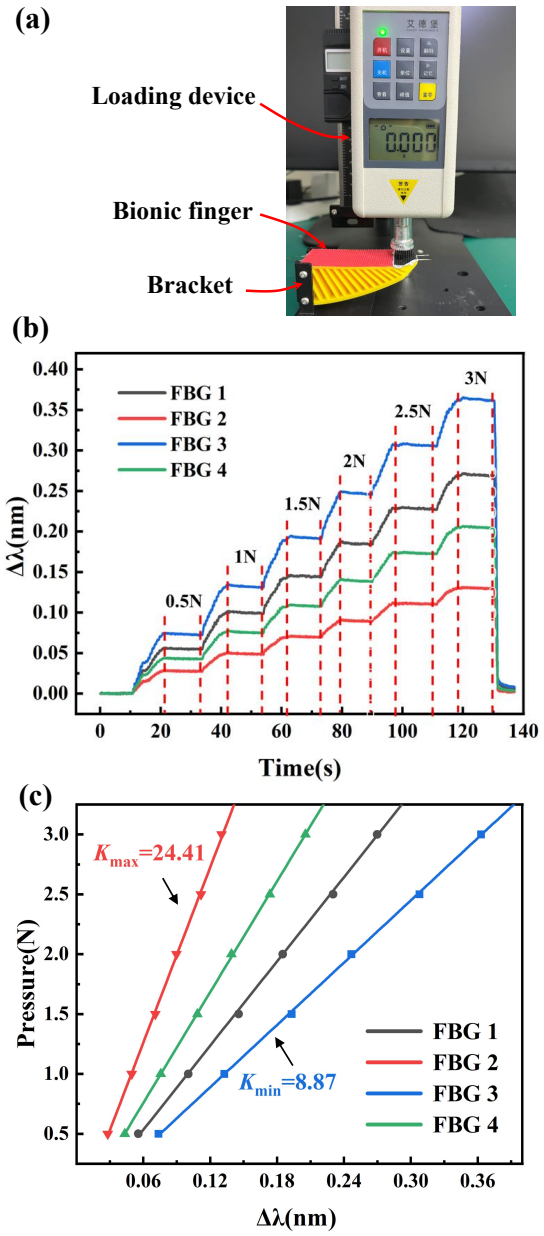

Fig. 5. (a) Pressure measuring system. (b) Variation of wavelength shifts under different pressure. (c) Relationship between normal pressure and wavelength shifts.

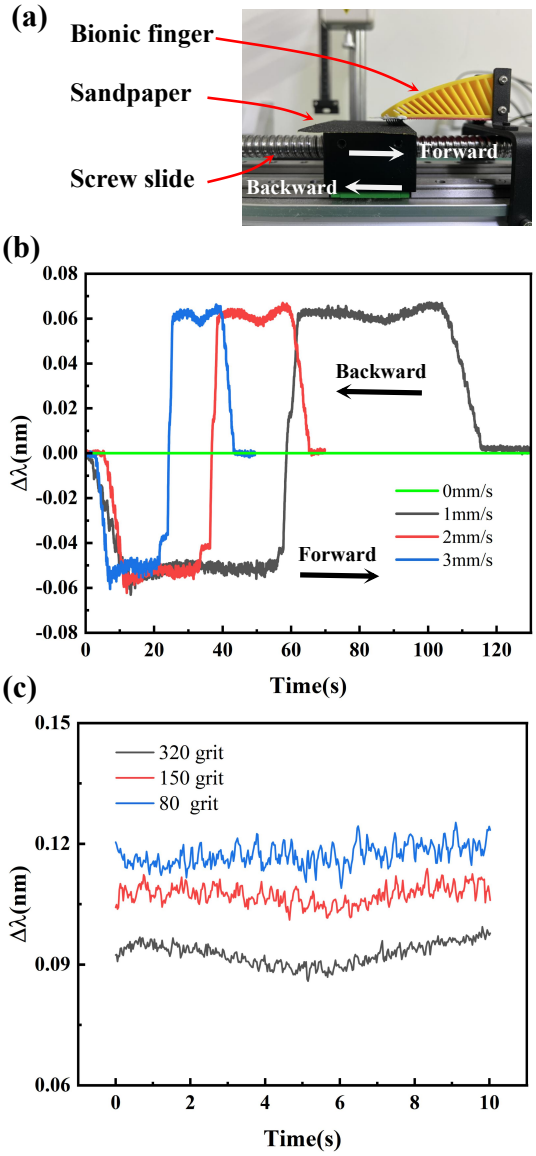

Fig. 6. (a) The Construction of a roughness testing platform. (b) The relationship beweent different speed and the wavelength shift of FBG 1. (c) The relationship beweent different rougness and the wavelength shift of FBG 3.

Furthermore, the positive and negative values of the wavelength drift can serve to identify the direction of fingertip touch. Experimental findings (Figure 6(c)) indicate that, with constant fingertip pressure, the wavelength drifts of FBGs (e.g., FBG 3) vary across different surface roughnesses. Upon the fingertip sequentially making contact with 320-grit, 150-grit, and 80-grit sandpaper, the corresponding wavelength drifts for FBG 3 are recorded as 0.09 nm, 0.1 nm, and 0.12 nm, respectively.

C. A soft robotic gripper with tactile sensing

1) Integration of sensing and control: As depicted in Figure 7(a), the parallel two-finger grasping system comprises two bionic fingers. This experiment primarily showcases the seamless integration of sensing and control within this system. The grasping system is powered by a stepper motor and meticulously governed by a computer operating at a baud rate of 11520. From Figure 7(b), the wavelength drift of FBG 7 acts as the pivotal signal for the motor's start-stop control, governed by two distinct thresholds (-0.15 nm and -0.19 nm). Threshold 1 discerns whether the gripper has effectively grasped the object, while threshold 2 determines the requisite firmness of the grip. FBG 1, representing the wavelength drift of W1, regulates the motor's function, with a threshold set at 0.01 nm.

Initially, the motor is set a initial position 850 step at a controlled speed of 10 steps/s. Subsequently, the gripper gradually approaches a transparent hollow sphere (30

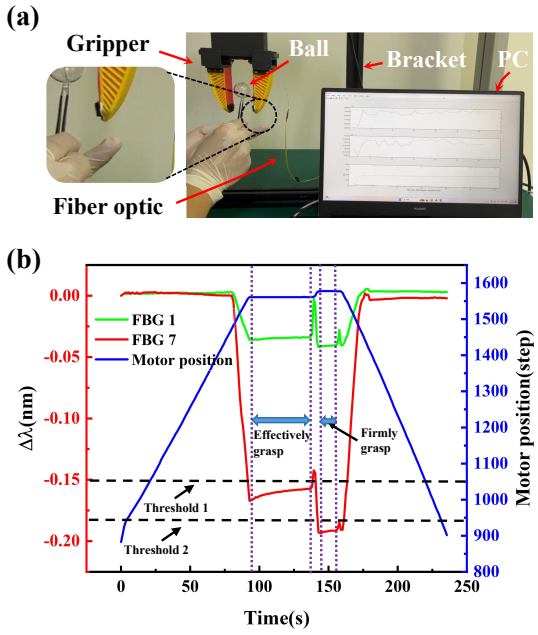

Fig. 7. (a)The parallel two-finger grasping system. (b) The process of sensing and control.

mm in diameter) to initiate the grasping action. Upon the wavelength drift of FBG 7 surpassing threshold 1 (at 135s), signifying successful ball grasping, the motor promptly halts. Concurrently, engagement of W1 (at 135s) and the subsequent exceeding of the 0.01 nm threshold in the wavelength drift of FBG 1 triggers the motor to resume operation, ensuring a more secure grip. Once the wavelength drift of FBG 7 surpasses threshold 2, indicating a firm hold on the ball, the motor ceases operation. Subsequent engagement of W1 (at 156s) initiates the release process. If the wavelength drift of FBG 1 exceeds 0.01 nm, the motor commences operation at a speed of -10 steps/s, allowing the gripper to gently release the ball.

2) Size recognition: This experiment aims to validate the soft gripper's ability to discern object size. FBG 5 - FBG 12, distributed within the bionic finger, serve as tactile sensors for grasping (Fig. 8(a)). Using a two-finger parallel gripper, acrylic hollow balls with diameters of 20mm, 30mm, 40mm, and 50mm are grasped. The threshold for FBG 7 is set at 0.15nm. Under stable grasping conditions, the wavelength drifts of each FBG sensor are recorded, and the average wavelength shift of each FBG is calculated. Consequently, eight average wavelength drifts serve as features to determine the size of the balls. Each ball is grasped 10 times, resulting in a total of 40 data sets.

A Convolutional Neural Network (CNN) model is constructed to classify the different balls. The CNN algorithm offer significant advantages in the recognition and classification of nonlinear problems. As depicted in Figure 8(b), the confusion matrix demonstrates that the accuracy of ball recognition using CNN reaches 100%.

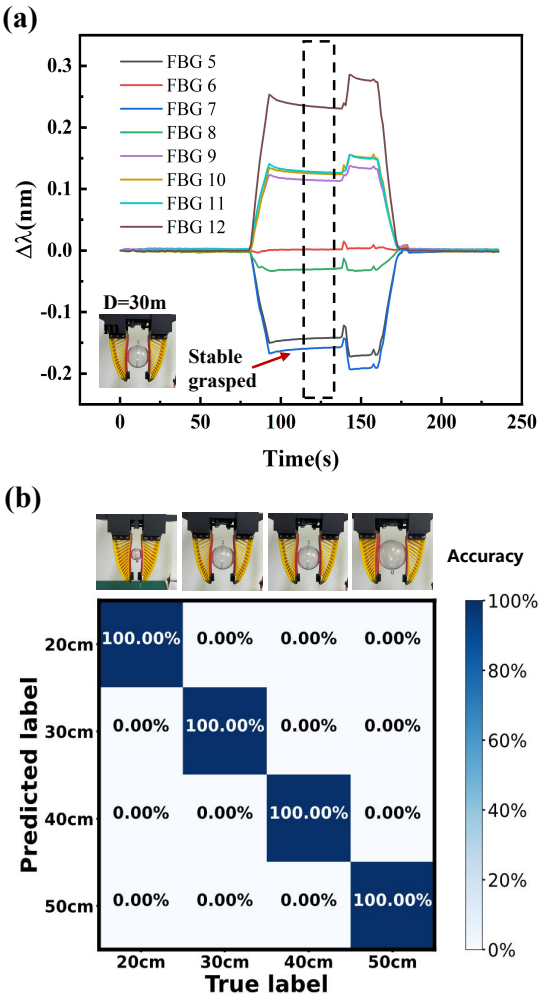

Fig. 8. (a) The wavelength shifts of FBG 5 - FBG 12. (b) The confusion matrix of ball recognition based on a CNN model.

V. CONCLUSION

In this study, inspired by various biological tactile mechanisms, we introduce a novel soft robotic finger design with biomimetic rat whiskers and hairs. Employing 3D printing and silicone coating techniques, we embedded distributed optical fiber sensors as tactile neurons within the biomimetic finger, forming a robust and compact multimodal sensing system. This tactile sensing system offers multimodal perception and high integration and reliability. This innovative finger can detect obstacles and their touch directions, measure fingertip forces, assess object surface roughness, and identify different curvatures(achieving up to 100% accuracy). Such advancements hold promise for diverse applications, including human-robot interaction in unstructured environments, precise manipulations, and tasks such as fruit sorting.

However, our study remains somewhat limited. Future research could focus on collecting additional data to enhance the precision of tactile roughness recognition. Furthermore, exploring the capacity of finger sensors to discern object slippage and stiffness during manipulation presents a promising avenue for further scholarly inquiry.

REFERENCES

[1] F. Ahmed, M. Waqas, B. Jawed, A. M. Soomro, S. Kumar, A. Hina, U. Khan, K. H. Kim, and K. H. Choi, "Decade of bio-inspired soft robots: A review," *Smart Materials and Structures*, vol. 31, no. 7, p. 073002, 2022.

[2] P. D. Marasco, J. S. Hebert, J. W. Sensinger, D. T. Beckler, Z. C. Thumser, A. W. Shehata, H. E. Williams, and K. R. Wilson, "Neurorobotic fusion of prosthetic touch, kinesthesia, and movement in bionic upper limbs promotes intrinsic brain behaviors," *Science Robotics*, vol. 6, no. 58, p. eabf3368, 2021.

[3] S. Zhang, B. Zhang, D. Zhao, Q. Gao, Z. L. Wang, and T. Cheng, "Nondestructive dimension sorting by soft robotic grippers integrated with triboelectric sensor," *ACS nano*, vol. 16, no. 2, pp. 3008–3016, 2022.

[4] M. Liu, Y. Zhang, J. Wang, N. Qin, H. Yang, K. Sun, J. Hao, L. Shu, J. Liu, Q. Chen, *et al.*, "A star-nose-like tactile-olfactory bionic sensing array for robust object recognition in non-visual environments," *Nature Communications*, vol. 13, no. 1, pp. 1–10, 2022.

[5] W. Liu, Y. Duo, J. Liu, F. Yuan, L. Li, L. Li, G. Wang, B. Chen, S. Wang, H. Yang, *et al.*, "Touchless interactive teaching of soft robots through flexible bimodal sensory interfaces," *Nature communications*, vol. 13, no. 1, pp. 1–14, 2022.

[6] J. Qu, B. Mao, Z. Li, Y. Xu, K. Zhou, X. Cao, Q. Fan, M. Xu, B. Liang, H. Liu, *et al.*, "Recent progress in advanced tactile sensing technologies for soft grippers," *Advanced Functional Materials*, p. 2306249, 2023.

[7] Y. Hao, Z. Liu, J. Liu, X. Fang, B. Fang, S. Nie, Y. Guan, F. Sun, T. Wang, and L. Wen, "A soft gripper with programmable effective length, tactile and curvature sensory feedback," *Smart Materials and Structures*, vol. 29, no. 3, p. 035006, 2020.

[8] J. Huang and A. Rosendo, "Variable stiffness object recognition with a cnn-bayes classifier on a soft gripper," *Soft robotics*, vol. 9, no. 6, pp. 1220–1231, 2022.

[9] M. Malekzadeh and F. N. Catbas, "A comparative evaluation of two statistical analysis methods for damage detection using fibre optic sensor data," *International Journal of Reliability and Safety*, vol. 8, no. 2-4, pp. 135–155, 2014.

[10] K. Hu, Z. Yao, Y. Wu, Y. Xu, X. Wang, and C. Wang, "Application of fbg sensor to safety monitoring of mine shaft lining structure," *Sensors*, vol. 22, no. 13, p. 4838, 2022.

[11] D. L. Presti, C. Massaroni, J. D'Abbraccio, L. Massari, M. Caponero, U. G. Longo, D. Formica, C. M. Oddo, and E. Schena, "Wearable system based on flexible fbg for respiratory and cardiac monitoring," *IEEE Sensors Journal*, vol. 19, no. 17, pp. 7391–7398, 2019.

[12] S. Li, X. Yin, C. Xia, L. Ye, X. Wang, and B. Liang, "Tata: A universal jamming gripper with high-quality tactile perception and its application to underwater manipulation," in *2022 International Conference on Robotics and Automation (ICRA)*. IEEE, 2022, pp. 6151–6157.

[13] Z. Xie, F. Yuan, Z. Liu, Z. Sun, E. M. Knubben, and L. Wen, "A proprioceptive soft tentacle gripper based on crosswise stretchable sensors," *IEEE/ASME transactions on mechatronics*, vol. 25, no. 4, pp. 1841–1850, 2020.

[14] Y. Luo, K. Wu, A. Spielberg, M. Foshey, D. Rus, T. Palacios, and W. Matusik, "Digital fabrication of pneumatic actuators with integrated sensing by machine knitting," in *CHI Conference on Human Factors in Computing Systems*, 2022, pp. 1–13.

[15] Z. Sun, S. Wang, Y. Zhao, Z. Zhong, and L. Zuo, "Discriminating soft actuators' thermal stimuli and mechanical deformation by hydrogel sensors and machine learning," *Advanced Intelligent Systems*, vol. 4, no. 9, p. 2200089, 2022.

[16] S. Dilibal, H. Sahin, J. O. Danquah, M. O. F. Emon, and J.-W. Choi, "Additively manufactured custom soft gripper with embedded soft force sensors for an industrial robot," *International Journal of Precision Engineering and Manufacturing*, vol. 22, no. 4, pp. 709–718, 2021.

[17] Z. Shen, Z. Zhang, N. Zhang, J. Li, P. Zhou, F. Hu, Y. Rong, B. Lu, and G. Gu, "High-stretchability, ultralow-hysteresis conductingpolymer hydrogel strain sensors for soft machines," *Advanced Materials*, vol. 34, no. 32, p. 2203650, 2022.

[18] M. Yang, Q. Liu, H. S. Naqawe, and M. P. Fok, "Movement detection in soft robotic gripper using sinusoidally embedded fiber optic sensor," *Sensors*, vol. 20, no. 5, p. 1312, 2020.

[19] P. Tripicchio, S. D'Avella, C. A. Avizzano, F. Di Pasquale, and P. Velha, "On the integration of fbg sensing technology into robotic grippers," *The International Journal of Advanced Manufacturing Technology*, vol. 111, no. 3, pp. 1173–1185, 2020.

[20] Y.-L. Park, K. Chau, R. J. Black, and M. R. Cutkosky, "Force sensing robot fingers using embedded fiber bragg grating sensors and shape deposition manufacturing," in *Proceedings 2007 IEEE International Conference on Robotics and Automation*. IEEE, 2007, pp. 1510–1516.

[21] Y.-L. Park, S. C. Ryu, R. J. Black, K. K. Chau, B. Moslehi, and M. R. Cutkosky, "Exoskeletal force-sensing end-effectors with embedded optical fiber-bragg-grating sensors," *IEEE Transactions on Robotics*, vol. 25, no. 6, pp. 1319–1331, 2009.

[22] J. I. Kim, D. Kim, M. Krebs, Y. S. Park, and Y.-L. Park, "Force sensitive robotic end-effector using embedded fiber optics and deep learning characterization for dexterous remote manipulation," *IEEE Robotics and Automation Letters*, vol. 4, no. 4, pp. 3481–3488, 2019.

[23] J. Feng and Q. Jiang, "Slip and roughness detection of robotic fingertip based on fbg," *Sensors and Actuators A: Physical*, vol. 287, pp. 143–149, 2019.

[24] L. Massari, C. M. Oddo, E. Sinibaldi, R. Detry, J. Bowkett, and K. C. Carpenter, "Tactile sensing and control of robotic manipulator integrating fiber bragg grating strain-sensor," *Frontiers in neurorobotics*, vol. 13, p. 8, 2019.

[25] Y. Hsu, L. Wang, W.-F. Liu, and Y. Chiang, "Temperature compensation of optical fiber bragg grating pressure sensor," *IEEE Photonics Technology Letters*, vol. 18, no. 7, pp. 874–876, 2006.

[26] J. L. Tangorra, G. V. Lauder, I. W. Hunter, R. Mittal, P. G. Madden, and M. Bozkurttas, "The effect of fin ray flexural rigidity on the propulsive forces generated by a biorobotic fish pectoral fin," *Journal of Experimental Biology*, vol. 213, no. 23, pp. 4043–4054, 2010.

[27] W. Crooks, S. Rozen-Levy, B. Trimmer, C. Rogers, and W. Messner, "Passive gripper inspired by manduca sexta and the fin ray® effect," *International Journal of Advanced Robotic Systems*, vol. 14, no. 4, p. 1729881417721155, 2017.

[28] K. Elgeneidy, A. Fansa, I. Hussain, and K. Goher, "Structural optimization of adaptive soft fin ray fingers with variable stiffening capability," in *2020 3rd IEEE International Conference on Soft Robotics (RoboSoft)*. IEEE, 2020, pp. 779–784.

[29] W. Crooks, G. Vukasin, M. O'Sullivan, W. Messner, and C. Rogers, "Fin ray® effect inspired soft robotic gripper: From the robosoft grand challenge toward optimization," *Frontiers in Robotics and AI*, vol. 3, p. 70, 2016.

[30] L. Massari, E. Schena, C. Massaroni, P. Saccomandi, A. Menciassi, E. Sinibaldi, and C. M. Oddo, "A machine-learning-based approach to solve both contact location and force in soft material tactile sensors," *Soft robotics*, vol. 7, no. 4, pp. 409–420, 2020.